Treatment Effect of Co(II) Coordination Polymer in Hypotension After Anesthesia by Regulating the Expression of α-Receptors

De-Gong LIU [1] & Jing-Yi ZHANG [2] *

[1] *Anesthesia Department, Yantai Yuhuangding Hospital,*
Yantai, Shandong, China
[2] *Anesthesia Department, The Second Hospital of Xi'an Medical Hospital,*
Xi'an, Shaanxi, China

SUMMARY. A new 1D Co(II)-containing coordination polymer (CP) with the chemical composition of $[Co(cptpy)Cl(H_2O)(DMF)]_n$ (**1**) has been prepared by the assembly of $CoCl_2·2H_2O$ with Hcptpy (Hcptpy = 4-(4-carboxyphenyl)-2,2':4',4'-terpyridine) under the solvothermal synthesis condition. The as-prepared coordination polymer **1** has been structurally characterized by different methods including X-ray single-crystal diffraction, elemental analysis, infrared (IR) spectrum, thermogravimetric (TG) analysis, and powder X-ray diffraction (PXRD). To prevent the hypotension after anesthesia, the relative expression of α receptors on peripheral small blood vessels was determined with real time RT-PCR. Then, the blood pressure of the animal was measured with non-invasive blood pressure monitor.

RESUMEN. Se ha preparado un nuevo polímero de coordinación (CP) que contiene Co(II) 1D con la composición química de $[Co(cptpy)Cl(H_2O)(DMF)]_n$ (**1**) mediante el ensamblaje de $CoCl_2$ $2H_2O$ con Hcptpy (Hcptpy = 4-(4-carboxifenil)-2,2':4',4''-terpiridina) en las condiciones de síntesis solvotérmica. El polímero de coordinación **1** tal como se preparó se ha caracterizado estructuralmente por diferentes métodos que incluyen difracción monocristalina de rayos X, análisis elemental, espectro infrarrojo (IR), análisis termogravimétrico (TG) y difracción de rayos X en polvo (PXRD). Para prevenir la hipotensión después de la anestesia, se determinó la expresión relativa de los receptores α en los vasos sanguíneos pequeños periféricos con RT-PCR en tiempo real. Luego, se midió la presión arterial del animal con un monitor de presión arterial no invasivo.

INTRODUCTION

There are many reasons for hypotension during anesthesia. The common reason is a drop in blood pressure caused by deep anesthesia [1]. Especially in patients with hypovolemia before anesthesia, intraoperative hypotension is more obvious. Anesthetic drugs cause allergies in patients, and the adrenal cortex is low, which leads to hypotension [2].

Medicinal inorganic chemistry has been stimulated by successes of platinum anticancer drugs that currently used as a component of nearly 50% of all cancer treatments [3]. Since the Rosenberg's breakthrough of the cisplatin antitumor activity, many metal-containing drugs based on platinum, palladium, tin, ruthenium, gold, rhenium and other metals have been designed for diagnostic and/or therapeutic purposes in disease therapy, some of them are in preclinical and clinical trials [4-6]. Among the series of compounds fabricated, the functional complexes attract great attention due to the potential drug value applications [7,8]. Thus, selecting safe, efficient and biocompatible ligands has become a crucial factor in the field of structural design, drug therapy and clinical applications. Polydentate ligands such as polycarboxylic acids or nitrogen-containing heterocyclic ligands are widely used in the rational design and controlled synthesis of these multifunctional complexes [9-12]. Recently, N-heterocyclic carboxylate ligands have attracted considerable attention of chemists and biologists because of their abundant

---

ISSN 0326 2383 (printed ed.)
ISSN 2362-3853 (on line ed.)

2927

coordination modes and functional properties, as well as hydrogen - bonding donors and acceptors under solution conditions [13-17].

In this study, a new 1D Co(II)-containing coordination polymer (CP) with the chemical composition of [Co(cptpy)Cl(H$_2$O)(DMF)]$_n$ (**1**) has been prepared by the assembly of Co-Cl$_2$·2H$_2$O with Hcptpy (Hcptpy = 4-(4-carboxy-phenyl)-2,2':4',4'-terpyridine) under the solvothermal synthesis condition. The as-prepared coordination polymer **1** has been structurally characterized by different methods including X-ray single-crystal diffraction, elemental analysis, infrared (IR) spectrum, thermogravimetric (TG) analysis, and powder X-ray diffraction (PXRD). Furthermore, the application values of the new compound were assessed through serial biological experiments. -

MATERIAL AND METHODS
Chemicals and measurements

All reagents are of analytical quality, used without further purification. Elemental analysis (C, H, N) was taken on a PerkinElmer 2400LS II elemental analyzer. IR spectra were recorded on a TENSOR 27 spectrophotometer in the range of 4000-400 cm^{-1}. Powder X-ray diffractograms were recorded with a Bruker SMART D8 Advance X-ray diffractometer using Cu Kα radiation (λ = 1.5406 Å) at 40 kV and 30 mA.

Preparation and characterization for [Co(cptpy)Cl(H$_2$O)(DMF)]$_n$ (1)

A mixture of CoCl$_2$·4H$_2$O (0.046 g, 0.20 mmol) and Hcptpy (0.0353 g, 0.10 mmol) was added in the 4.0 mL of mixed solvents of DMF (2.0 mL) and H$_2$O (2.0 mL), then the mixture was sealed in a 20 mL screw capped vial and placed in an oven at 100 °C for 5 d. Pink strip crystals were obtained in ca. 62% yield (based on Hcptpy). Elemental analysis calcd (%) for C$_{25}$H$_{23}$CoClN$_4$O$_4$: C, 55.83; H, 4.31; N, 10.42. Found: C 56.02, H 4.25, N 10.58. IR (KBr pellets): 3356 (br), 3064 (w), 1655 (s), 1594 (s), 1545 (w), 1395 (s), 1251 (w), 1223 (w), 1196 (w), 1113 (m), 1064 (m), 1018 (m), 993 (w), 864 (w), 830 (m), 790 (s), 739 (w), 704 (m), 676 (m), 625 (m), 514 (m), and 483 (m) cm^{-1}.

The X-ray data were obtained by utilizing the Oxford Xcalibur E diffractometer. The intensity data was analyzed by utilizing the CrysAlisPro software and converted to the HKL files. The SHELXS program on the basis of direct approach was utilized to create the initial structural models, and the SHELXL-2014 program on the basis of the least-squares approach was modified. The whole

Empirical formula	C$_{25}$H$_{23}$ClCoN$_4$O$_4$
Formula weight	537.85
Temperature/K	98.04
Crystal system	triclinic
Space group	P-1
a/Å	7.4632(11)
b/Å	11.2578(12)
c/Å	15.7412(17)
α/°	93.628(3)
β/°	98.7410(10)
γ/°	104.632(4)
Volume/Å^3	1257.6(3)
Z	2
ϱ$_{calc}$ g/cm^3	1.420
μ/mm^{-1}	0.827
Reflections collected	11352
Independent reflections	4357 [R$_{int}$ = 0.0374, R$_{sigma}$ = 0.0485]
Data/restraints/parameters	4357/2/323
Goodness-of-fit on F^2	1.044
Final R indexes [I>=2σ (I)]	R$_1$ = 0.0716, ωR$_2$ = 0.2068
Final R indexes [all data]	R$_1$ = 0.1106, ωR$_2$ = 0.2384
Largest diff. peak/hole / e Å^{-3}	1.17/-0.43
CCDC	2113680

Table 1. Refinement details and crystallographic parameters for complex **1**.

non-H atoms were mixed with anisotropic parameters. Then we utilized the AFIX commands to fix the whole H atoms geometrically on the C atoms that they attached. Table 1 details refinement details as well as crystallographic parameters of the complex **1**.

Real time RT-PCR

After the synthesis of the new compound, its inhibitory activity on the relative expression of the α receptor expression on the vascular endothelial cells was measured with the real time RT-PCR. This preformation was conducted in accordance with the protocols with only a little modification. In brief, the 50 animals with 4-5 weeks old and 20-22 g weight were used in this present research, which were purchased from the Nanjing University (Nanjing, China), and kept in the standard condition with 20-25 °C which free water and food. The anesthesia operation was conducted on the animal and the new compound was given for treatment at the concentration of 1, 2, and 5 mg/kg. After the indicated treatment, the vascular endothelial cells were isolated and harvested from all the animals. Then, the total RNA in the

cells were extracted and the concentration of the total RNA was measured with OD260/OD280. Next, the total RNA was reverse transcribed into cDNA. Finally, the expression levels of α receptor expression on the vascular endothelial cells was determined. The *gapdh* was used as the control gene. This preformation was conducted at least three times, and the results were presented as mean ± SD.

Blood pressure measurement

To evaluate the biological activity of the compound with novel structure, the blood pressure of the animal after treatment was measured with the non-invasive blood pressure monitor. This preformation was conducted totally under the guidance of the instructions with only a little change. Briefly, 50 animals with 4-5 weeks old and 20-22 g weight were used in this present research, which were purchased from the Nanjing University (Nanjing, China), and kept in the standard condition with 20-25 °C, which free water and food. The anesthesia operation was conducted on the animal and the new compound was given for treatment at the concentration of 1, 2, and 5 mg/kg. After the indicated treatment, the blood pressure of the animal was determined with non-invasive blood pressure monitor blood pressure

monitoring. This preformation was conducted at least three times, and the results were presented as mean ± SD.

RESULTS AND DISCUSSION
Structural characterization

Single-crystal structural analyses demonstrate that **1** crystallizes in the triclinic space group *P*-1. The asymmetric skeleton contains one Co^{2+} ion, one cptpy$^-$ ligand, one Cl$^-$ anion, one coordinated H_2O and one coordinated DMF molecule (Fig. 1a), generating the formula as follows, [Co(cptpy)Cl(H_2O)(DMF)]$_n$. Each six-coordinated Co^{2+} ion in **1** adopts the distorted octahedron geometry, which is defined by one Cl atom, one N atom of cptpy$^-$ ligand, and four O atoms, the four O atoms from two carboxyl O atoms of one cptpy$^-$ ligand through the chelating mode, one H_2O, and one DMF molecule, respectively. In the coordination configuration of Co^{2+} ion (Fig. 1b), the O1, O2, N3 and O4 atoms constitute the middle section of the octahedron, and Cl1 and O3 atoms severally locate the two vertexes of the octahedron. The standard deviation from the least-square of the middle section is 0.069 Å, the distance between Co1 and the section is 0.1324 Å, and the distances between Cl1 and O3 atoms and the middle section are 2.6763 and 2.0473 Å, respectively. The
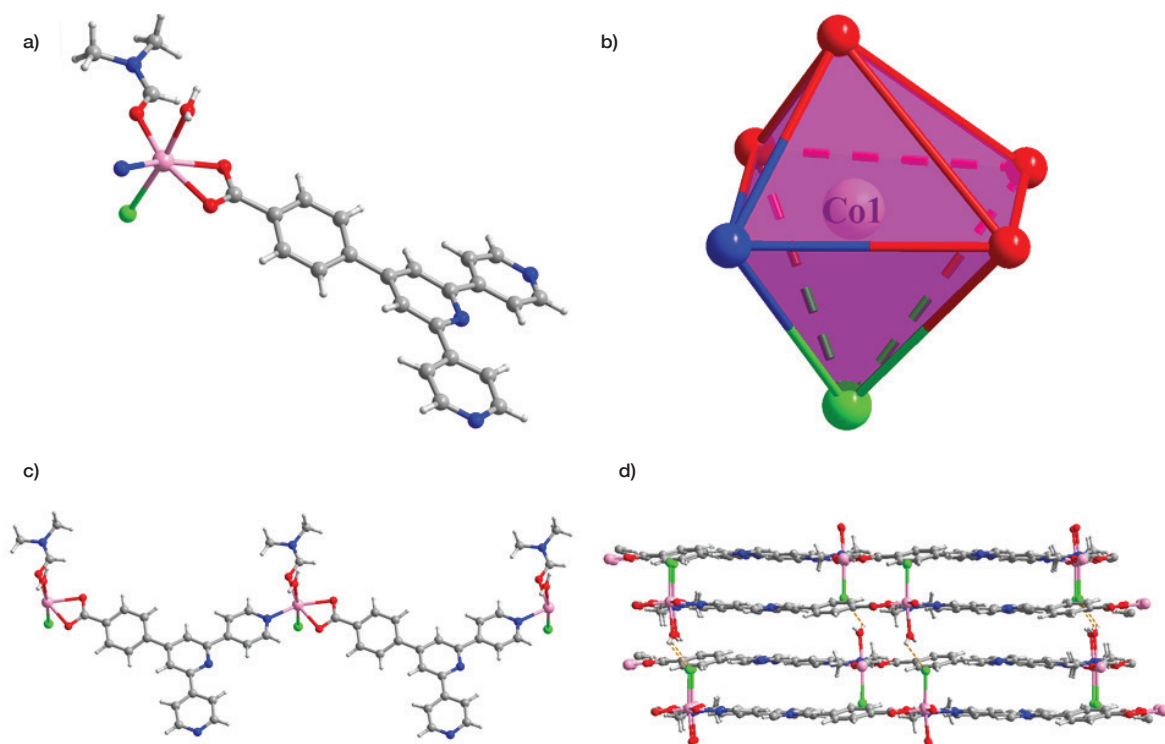

Figure 1. (**a**) The least building unit of **1**. (**b**) The coordination pattern for the Co ion. (**c**) The D chain of **1**. (**d**) 3D H-bond network of **1**.
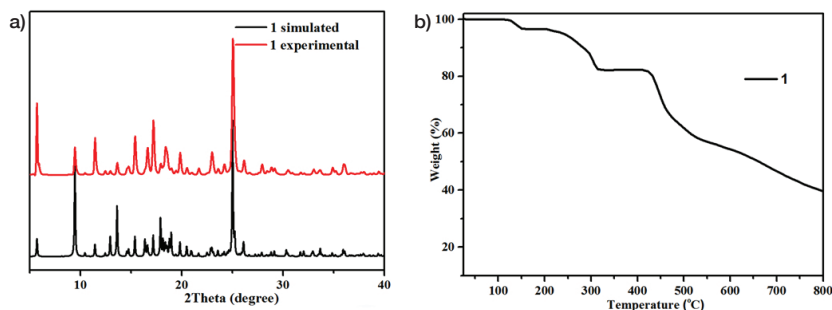
Figure 2. (**a**) The PXRD patterns for **1**. (**b**) The TGA curve for **1**.

Cl1, O2, and N3 atoms, the Cl1, O1, and O2 atoms, the Cl1, O1, and O4 atoms, the Cl1, O4, and N3 atoms, the O3, O2, and N3 atoms, the O3, O1, and O2 atoms, the O3, O1, and O4 atoms, the O3, O4, and N3 atoms, severally constitute the eight sides of the octahedron. The dihedral angles between the eight sides and the middle section are 59.0°, 127.4°, 116.5°, 65.2°, 127.7°, 55.8°, 43.6°, and 119.2°, and the distances between Co1 and the eight sides are 1.2518, 1.4775, 1.1655, 1.1472, 1.2844, 1.2188, 1.4530, and 1.2204 Å, respectively. The above data indicate that the octahedron is appreciably distorted. Adjacent Co^{2+} ions are alternately bridged by carboxyl O atoms and pyridine N atoms of cptpy$^-$ ligands to generate a 1D chain (Fig. 1c), which could be further stacked to produce a 3D supramolecular structure through hydrogen bonds and $\varpi\cdots\varpi$ stacking interactions (Fig. 1d).

To check the phase purity of the products, powder X-ray diffraction (PXRD) experiments have been carried out for these complexes (Fig. 2a). The peak positions of the experimental and simulated PXRD patterns are in good agreement with each other, indicating that the crystal structure is truly representative of the bulk crystal products. The differences in intensity may be owing to the preferred orientation of the crystal samples. To confirm the thermal stability of **1**, the thermal stability of **1** was executed under the N_2 atmosphere in the range of 25-1000 °C (Fig. 2b). The TG curve of **1** shows a two-step weight loss process, the first weight loss of 3.15% between 25 and 150 °C corresponds to the remove of one coordinated water molecule (calcd. 3.35%), the second weight loss of 13.62% from 150 to 320 °C could be attributed to the decomposition of one coordinated DMF molecule (calcd. 13.59%).

Compound significantly reduced the relative expression of the α receptor expression on the vascular endothelial cells

After the synthesis of the compound with novel structure, its application value on the hypotension after anesthesia was assessed, the mechanism of the compound was explored at the same time. As the α receptor mainly exist on the vascular endothelial cells, which is important in the blood pressure maintaining. So, the real time RT-PCR was further conducted and the relative expression levels of the α receptor expression on the vascular endothelial cells was determined after indicated compound treatment. As the results showed in Fig. 3, we can see that, in the hypotension group, there was a much lower level of blood pressure compared with the control group. After the treatment of the new compound was levels of the α receptor expression on the vascular endothelial cells was increased in a dose and time dependent manner.
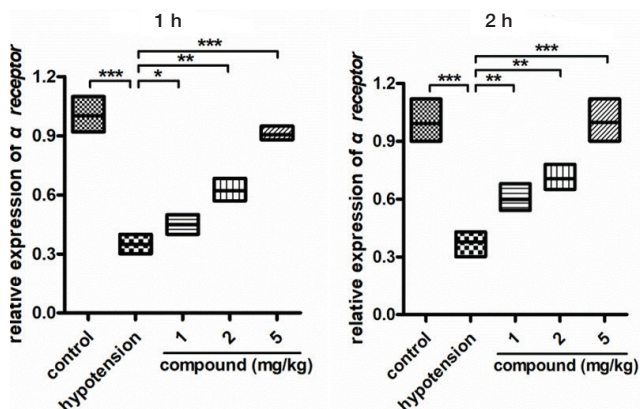

Figure 3. Significantly reduced the relative expression of the α receptor expression on the vascular endothelial cells after compound treatment. The anesthesia operation was conducted on the animal and the new compound was given for treatment at the concentration of 1, 2, and 5 mg/kg. The real time RT-PCR assay was used to measure the relative expression of the α receptors on peripheral small blood vessels after compound treatment.
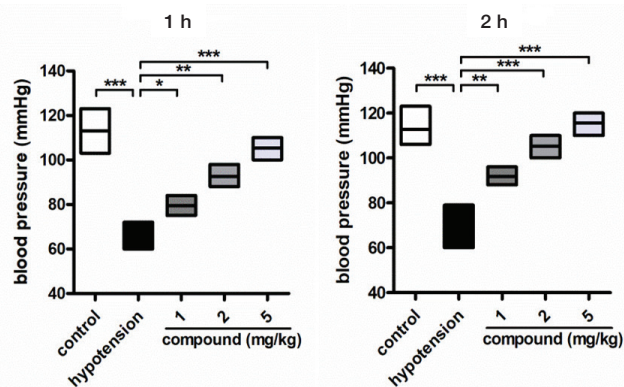
Figure 4. Compound obviously prevented the hypotension after anesthesia. The anesthesia operation was conducted on the animal and the new compound was given for treatment at the concentration of 1, 2, and 5 mg/kg. The blood pressure of the hypotension animal was determined at indicated time with non-invasive blood pressure monitor

Hypotension is prevented by the new compound significantly

In the above research, we have proved that the compound could significantly increase the relative expression of the α receptor expression on the vascular endothelial cells. In this research, the blood pressure of the hypotension animal under compound treatment was further measured. The results in Fig. 4 showed that in the model group, there was a significantly reduced level of blood pressure compared with the control group. After the treatment of the compound, the blood pressure of the animal was significantly increased, suggesting the obviously excellent application values of the compound on the preventing hypotension. This result suggested that the biological activity of the compound on preventing hypotension after anesthesia by regulating the expression of α receptors.

CONCLUSION

In summary, we have prepared a 1D Co(II)-containing coordination polymer by the assembly of $CoCl_2 \cdot 2H_2O$ with Hcptpy (Hcptpy = 4-(4-carboxyphenyl)-2,2':4',4'-terpyridine) under the solvothermal synthesis condition. The as-prepared coordination polymer **1** has been structurally characterized by different methods including X-ray single-crystal diffraction, elemental analysis, infrared (IR) spectrum, thermogravimetric (TG) analysis, and powder X-ray diffraction (PXRD). The results of the real time RT-PCR indicated that the compound could increase the elative expression of the α receptors on peripheral small blood vessels dose dependently. Next, the hypotension is also prevented by the new compound significantly. Finally, we got this conclusion, the new compound could be an excellent candidate for the hypotension therapy by stimulating the relative expression of the α receptors on peripheral small blood vessels in a dose dependent manner.

REFERENCES

1. Van de Velde, M. (2019) *Curr. Opin. Anaesthesiol.* **32**: 268-70.
2. Abukhouskaya, N., R. Kowalczyk, G. Górniewski, M. Janiak, D. Kosson & J. Trzebicki (2020) *Pol. Merkur. Lekarski.* **48**: 215-20.
3. Barry, N.P.E. & P.J. Sadler (2013) *Chem. Commun.* **49**: 5106-31.
4. Vojtek, M., M.P.M. Marques, I.M.P.L.V.O. Ferreira, H. Mota-Filipe & C. Diniz (2019) *Drug Discov. Today* **24**: 1044-–58.
5. Hu, M.L., S.A. Razavi, M. Piroozzadeh & A. Morsali (2020) *Inorg. Chem. Front.* **7**: 1598-632.
6. Hu, M.L., M. Y. Masoomi & A. Morsali (2019) *Coord. Chem. Rev.* **387**: 415-35.
7. Fan, L., D. Zhao, B. Li, F. Wang, Y. Deng, Y. Peng, *et al.* (2022) *Spectrochim. Acta A* **264**: 120232.
8. Fan, L., D. Zhao, H. Zhang, F. Wang, B. Li, L. Yang, *et al.* (2021) *Micropor. Mesopor. Mat.* **326**: 111396.
9. Li, R.F., X.F. Liu, T. Zhang, X.Y. Zhang & X. Feng (2014) *J. Mol. Struct.* **1075**: 456-61.
10. R.F. Li, Y.X. Gu, X.F. Liu, X. Feng & L.F. Ma (2015) *Z. Anorg. Allg. Chem.* **641**: 1114-8.
11. Feng, X., R.F. Li, L.Y. Wang, S.W. Ng, G.Z. Qin & L.F. Ma (2015) *CrystEngComm* **17**: 7878-87.
12. Wen, T., D.X. Zhang, J. Liu, R. Lin & J. Zhang (2013) *Chem. Commun.* **49**: 5660-2.
13. Zheng, L.N., F.H. Wei, H.M. Hu, C. Bai, X.L. Yang, X. Wang, *et al.* (2019) *Polyhedron* **161**: 47-55.
14. Pu, M., Y. Ma, J. Wan, Y. Wang, J. Wang & M.L. Brusseau (2017) *Catal. Sci. Technol.* **7**: 1129-40.
15. Feng, X., Y.Q. Feng, N. Guo, Y.L. Sun, T. Zhang, L.F. Ma, *et al.* (2017) *Inorg. Chem.* **56**: 1713-21.
16. Sen, R., A. Halder & D. Ghoshal (2020) *Polyhedron* **183**: 114534.
17. Zhang, H.M., Y.C. He, J. Yang, Y.Y. Liu & J.F. Ma (2014) *Cryst. Growth Des.* **14**: 2307-17.